

Original Research

NUMERICAL AND EXPERIMENTAL INVESTIGATION OF SEMICIRCULAR SOLAR UPDRAFT TOWER SYSTEM EMPLOYING POROUS COPPER METAL FOAM

Sarmad A. Abdul Hussein*, Mohammed A. Nima

Department of Mechanical Engineering, College of Engineering, University of Baghdad, Baghdad, Iraq
(<https://orcid.org/0000-0002-2923-7891>; <https://orcid.org/0000-0002-3107-5262>)

Received 02/07/2022

Accepted in revised form 31/10/2022

Published 01/09/2023

Abstract: The numerical and experimental study was carried out under Iraqi weather conditions to verify the improvement of the performance of the solar updraft tower system SUTS by introducing porous metal foam as a heat-absorbent plate. A semicircular basin of the solar collector was divided into two equal identical quarters. A porous foam material was fixed on one of the basins while the other basin was fixed on a traditional copper plate. The positions of the metal foam absorber plate are changed with two inclination angles (0° and 18°) and the optimum position is achieved when it gives the highest thermal performance. A finite volume modeling technique is used to solve the governing equations and radiation heat transfer equations by using ANSYS Fluent. The experimental part was conducted in Baghdad / Iraq at latitude 33.3° . The presence of the metal foam absorber plate caused a significant decrease in the average temperatures of the heat-absorbent plate. The maximum airflow temperature was recorded with an inclined angle of 18° . The metal foam as a heat-absorbent plate enhanced the efficiency and the output power of the SUTS to about 51.9% and 47.2% respectively compared to the traditional plate.

Keywords: Renewable energy; solar chimney power plant; Ansys fluent programming; porous metal foam

1. Introduction

The use of renewable energy at present time is an urgent necessity because it is of paramount importance to the economy of countries. One of

the most important types of renewable energy is the use of solar energy to generate energy. The use of solar chimneys to generate energy is one of the important techniques that are characterized by simplicity of work, ease of maintenance, and longevity of more than a hundred years [1-4]. The surface of the porous material overall and mineral metal foam, specifically, is described by having an exceptionally huge surface region where the proportion of the surface area to the process of heat transfer volume (500 to $10000 \text{ m}^2/\text{m}^3$) permits to enhance the transfer of heat largely from the heat absorbent surface to the flow of air inside the SUTS based gatherer and afterward increment of the air siphoning towards the solar updraft tower. Hence, the metal foam is utilized as a heat absorbent plate in the SUTS to expand the collector's thermal effectiveness because of the buoyancy force increment, so it will be affected directly by the performance of SUTS [5-7]. On this basis, many numerical and experimental researches have been carried out aimed at improving the performance of the solar tower system [8-9].

*Corresponding Author:
sarmad.alsaraf@coeng.uobaghdad.edu.iq

An analytical and numerical study was conducted by Johannes [10] to investigate the energy, generation by a large-scale, solar tower power plant. The results showed that the tower's height and the solar collector's diameter affected the annual electricity output. At the same time, energy production was increased by improving the shape and height of the collector roof. A theoretical investigation of a solar chimney was presented by Abdel Hamid et al. [11] to predict the behavior of the thermo-hydrodynamic of the solar chimney. The methodology showed that the optimal geometric and operational characteristics were directly affected by the characteristics of the airflow. Also, this study included the comparison between a straight shape and a curved shape of the chimney cover junction. He found that the curved junction was given a high flow compared with the straight junction. The heat and mass transfer models of the porous silicon carbide foam (SiC) solar receiver were applied by Chang et al. [12] to investigate numerically the effect of the porosity, diameter, thickness, and velocity of the air inlet, on the temperature distribution in china. The results showed that the higher porosity gave a lower temperature of the absorber surface and a higher temperature of the working fluid and as well as the bigger particle diameter was given a high temperature for solid surface and passing air inside the solar tower system. Elizabeth [13] studied the airflow in SCPP by using ANSYS FLUENT. He assumed that the chimney was located in sub-Saharan Africa and operated for 24 hours a day to simulate the night-time operation of the solar chimney. Results showed that using the thermal storage layer as a porous material is the best way to model the solar collector with a no-slip, mixed convective, and radiative boundary. The effect of the inclination angle of the collector roof on the SCPP performance was examined by Ehsan and Kim

[14] to study the effect of the collector design configuration on Manzanares power plant performance by using computational fluid dynamics. Results showed that the variability in the collector roof inclination affected the convection sample inside the solar collector which led to an increase in the mass flow rate of the SCPP. Xiping [15] designed and built the solar chimney power plant in China to consist of a collector diameter of 10 m and a chimney height of 8 m. Experimental investigation of a solar chimney prototype was conducted in Baghdad from August to November 2009 by Miqdam [16] The effect of the chimney's basement on the air collector and temperatures was studied. The glass collector roof was changed by a transparent plastic roof. Abdulcelil [17] designed and constructed the SUTS in adiyaman to investigate the distribution of the absorber and air temperatures. Mehrdad et al. [18] experimentally studied the solar tower performance by analyzing some of the factors such as heat absorbent plate and the effect of SUTS dimensions. The impact of pressure drop, solar collector angle, and airflow passing through the turbine fixed in the tower inlet was studied experimentally and numerically by Carl [19]. Aseel et al. [20] numerically and experimentally studied the effect of changing the height of the solar collector cover from the basin at different distances. Through the study, it became clear that the lower the cover height from the basin gives better results due to an increase in the airflow towards the solar tower. The effect of the inlet height of the collector on the SUTS was investigated by Mohammed et al. [21] under climate conditions of Karbala City/Iraq.

Although the numerical and experimental studies on the topic of the present problem are scarce or non-existent, some relevant experimental and

numerical investigations have been reported in the literature but for other types of porous medium. However, such speculation has not been verified experimentally or numerically that examined the possibility of enhancing the performance of SUTS by using the metal foam as a collector absorber plate inside the SUTS. The point of contribution in the present work is using porous copper foam as a heat-absorbent plate and investigating numerically and experimentally the effect of an inclination angle (0° and 18°) of porous absorber plate on the SUTS performance.

2. Numerical Simulations

2.1. Physical Description

The numerical analysis is presented for three-dimensional, two-quarter circular collectors, steady state, and natural convection heat transfer. Air was used as an ideal gas as the working fluid. Simulation of the buoyancy model was carried out by defining gravity (-g) in the (Y) direction. Use 1atm. as a reference air pressure. The simulation was performed with a flat and metal foam absorber plate at an inclination angle of the absorber plate. The ANSYS FLUENT provides the ability to model, mesh, give appropriate boundary conditions, and simulate them under Iraqi weather conditions to obtain results three-dimensional models were used to simulate the present study cases, passing through four steps: geometry formation, meshing, setup processing, and final analysis of results.

2.2. Governing Equations

The FLUENT program uses the basic three-dimensional fluid equations of airflow to maintain mass, momentum, and energy to calculate fluid properties [13]. After simplifications all of the equations (continuity, momentum, and energy) can be written as follows;

$$(\vec{\nabla} \cdot \vec{v}) = 0 \quad (1)$$

$$\vec{v} \cdot \vec{\nabla} \cdot \vec{v} = -\frac{1}{\rho_o} \vec{\nabla} P + \frac{\mu}{\rho_o} \vec{\nabla}^2 \vec{v} + \vec{g}[1 - \beta(T - T_o)] \quad (2)$$

$$\vec{v} \cdot \vec{\nabla} T = \alpha_f \vec{\nabla}^2 T \quad (3)$$

$$\text{Where; } \alpha_f = \frac{k_f}{\rho C_P}$$

The Boussinesq model assumed that the density of the fluid is a function of temperature and can be expressed throughout the coefficient of thermal expansion, β ,

$$\beta = -\frac{1}{\rho} \left(\frac{\partial \rho}{\partial T} \right)_P \quad (4)$$

Eq. 4 shows the fluid density was varied with temperature. Therefore, the change of the fluid temperature inside the tower system is small. The density of the fluid was expressed by the following equation;

$$(\rho - \rho_o) \approx -\rho_o \beta (T - T_o) \quad (5)$$

Eq. 5 uses in FLUENT ANSYS to estimate the fluid density which associates the buoyancy force in the momentum equation.

2.3. Formulation of Porous Copper Foam

The metal foam absorber plate model construes that the air moves between the pores particles and interacts with them. A pore model in the numerical simulation will add an additional source (\vec{S}) to the momentum equation [22];

$$\vec{S} = -\left(\frac{\mu}{a} \vec{\nabla} + C_F \frac{1}{2} \rho |\vec{V}| \vec{V} \right) \quad (6)$$

Eq. 6 consists two terms; the first represents Darcy term and the second is Forchheimer term. a and C_F represent the resistances of the metal foam to the air flow (permeability and the inertial drag factor) respectively and can be expressed by the following equations;

$$a = 0.00073(1 - \varepsilon)^{-0.224} \left(\frac{d_f}{d_p} \right)^{-1.11} (d_p)^2 \quad (7)$$

$$C_F = 0.00212(1 - \varepsilon)^{-0.132} \left(\frac{d_f}{d_p} \right)^{-0.163} \quad (8)$$

The porous absorber model modifies the energy equation to describe;

$$\vec{\nabla} \cdot (\vec{v} ((\rho_f E_f + P))) = S_f^h + \vec{\nabla} \cdot [k_{eff} \vec{\nabla} T - (\sum_i h J_i) + (\vec{\tau} \cdot \vec{v})] \quad (9)$$

Where, k_{eff} is the effective thermal conductivity and can be found from the below equation [23];

$$k_{eff} = \epsilon k_f + (1 - \epsilon) k_s \quad (10)$$

2.4. Modeling Geometry

The modeling geometry was generated and simulated by the FLUENT software program as shown in Fig. 1. The dimensions of the solar tower system are 2m radius of the quarter circular collector. The radius of the flat and metal foam absorber plate is 1.75 m. The thickness of the flat (copper) absorber plate is 1mm and the thickness of the metal foam absorber plate is 10 mm. The height of the air inlet is 3 cm. Height and diameter of the tower tube (3.5m and 6.5 cm) respectively. The tilted collector roof angle is 22.5°. Due to the turbulent airflow, the realizable $k-\epsilon$ was selected to determine the full buoyancy effect. The $k-\epsilon$ turbulence model assumed that the flow is wholly turbulent and the molecular viscosity effects are neglected. The realizable $k-\epsilon$ model used two equations to find the first one for specific turbulent kinetic energy (k) and the second for the turbulent dissipation rate (ϵ) [24], where;

$$\vec{\nabla} \cdot (\rho k \vec{v}) = \vec{\nabla} \cdot \left[\left(\mu + \frac{\mu_t}{\sigma_k} \right) \vec{k} \right] + G_k + G_{b_t} - \rho \epsilon$$

$$\vec{\nabla} \cdot (\rho \epsilon \vec{v}) = \vec{\nabla} \cdot \left[\left(\mu + \frac{\mu_t}{\sigma_\epsilon} \right) \vec{\epsilon} \right] + \rho C_1 S_\epsilon - \rho C_2 \frac{\epsilon^2}{k + \sqrt{\nu \epsilon}} + C_{1\epsilon} \frac{\epsilon}{k} C_{3\epsilon} G_b \quad (12)$$

The radiation model was applied in the present work. Due to the transparent media of the solar collector roof, the Discrete Ordinates (DO)

model is selected and can be expressed by the following equation [25];

$$\frac{dI(\vec{r}, \vec{s})}{ds} + (\alpha + \sigma_s) I(\vec{r}, \vec{s}) = \alpha n^2 \frac{\sigma T^4}{\pi} + \frac{\sigma_s}{4\pi} \int_0^{4\pi} I(\vec{r}, \vec{s}') \Phi(\vec{s}, \vec{s}') d\Omega' \quad (13)$$

Where $I(\vec{r}, \vec{s})$ is the intensity of radiation that is based on a position direction, α is the coefficient of the absorption, σ_s is the coefficient of the scattering, n is the refractive index, and σ is Stefan–Boltzmann constant.

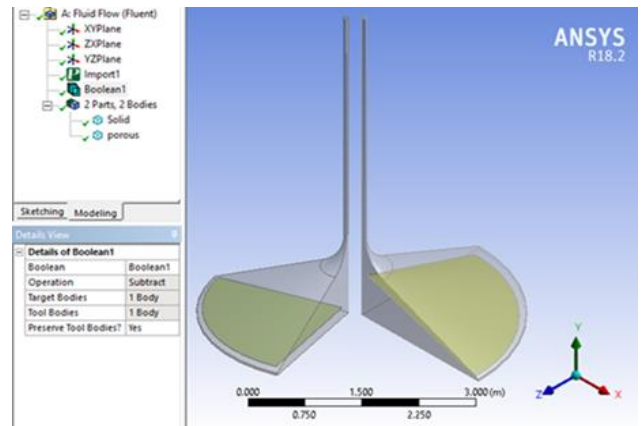


Figure 1. SUTS model coordinates with flat Plate ($\beta = 0^\circ$) and for copper foam absorption plate ($\beta = 18^\circ$)

2.5. Boundary Conditions

Fig. 2 shows all the boundary conditions for the numerical model. The porous jump condition is the best method to define the boundary condition for the metal foam absorber plate due to the thickness of the metal foam is very small compared to the radius of the metal foam [26]. Fig. 3 shows the porous jump condition of the metal foam absorber plate.

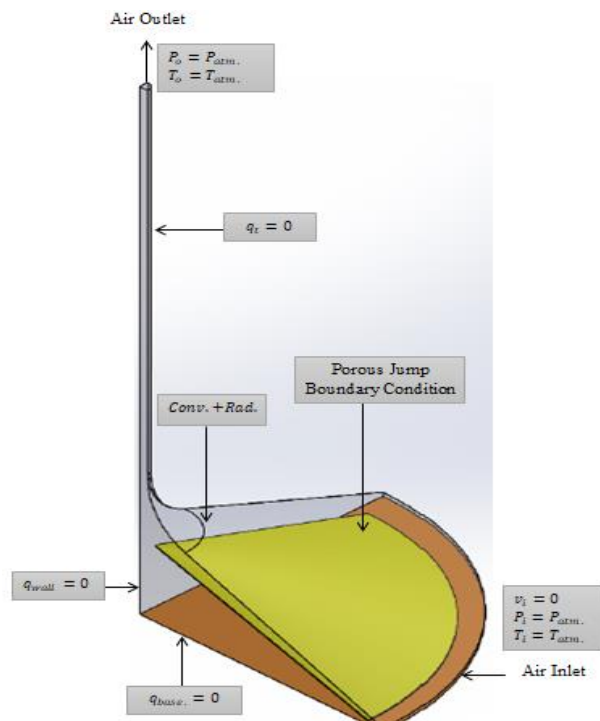


Figure 2. Boundary conditions of the used models

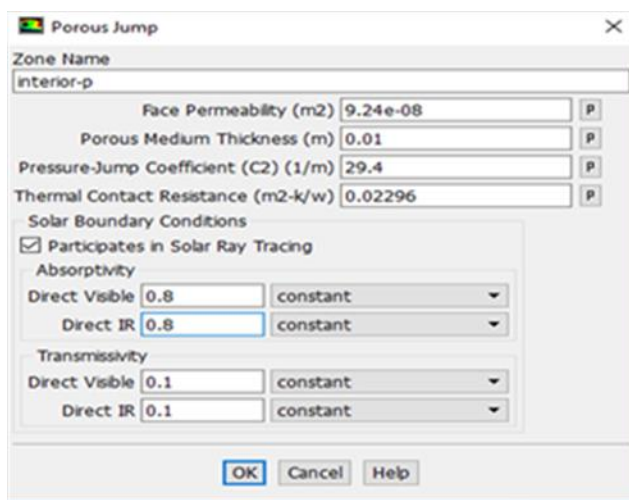


Figure 3. Porous jump boundary condition for copper foam absorption plate

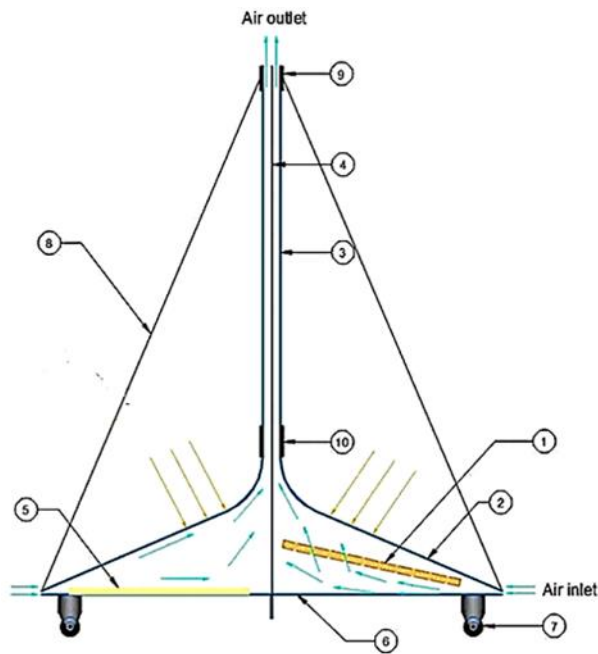
3. Experimental Set-up and Procedure

The practical apparatus included two separate, and identical solar updraft tower apparatus. The two SUTS were designed and manufactured;

each one consists of a quarter-round thermal solar collector and a long tube (tower). The aim of fabricating two identical SUTS is to investigate the SUTS performance through the comparison between the traditional flat plate and porous absorber under the same atmospheric conditions. Figs. 4 and 5 indicate the experimental device schematically and photographically.

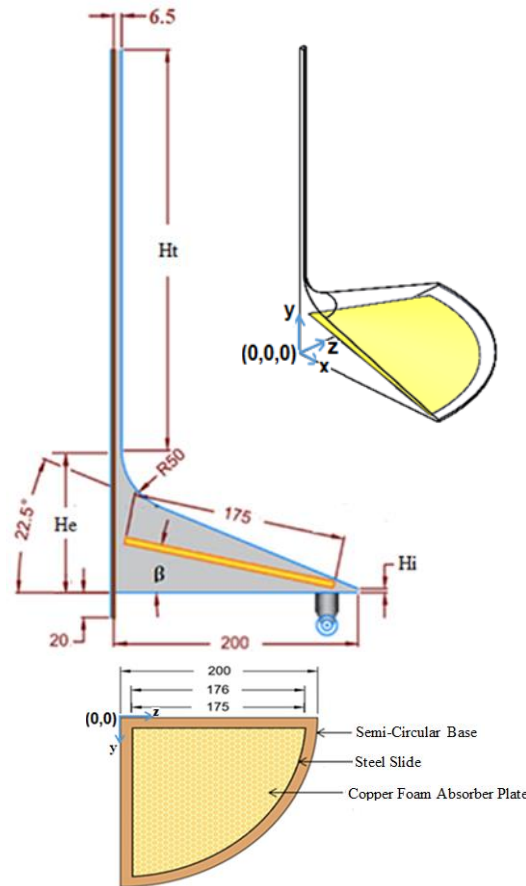
3.1. Solar Air Collector

Fig. 4 and Fig. 5 show the semicircular collector structure that was manufactured of a 4 m diameter to install the air solar collector. The semi-circular base of the solar collector was divided into two-quarter circles of equal size of a 2 m radius. The two-quarters of the solar collectors are separated from each other using a 20 mm thick wooden panel to isolate the collectors from each other tightly. The porous copper foam and the traditional flat plate were fixed on each base of the solar collector as two heat-absorbing surfaces. Each solar collector was covered by sheets made from acrylic transparent with a 2.5 mm thickness. A wooden door was manufactured for each solar collector with a thickness of 2 mm and a width of 2 m. It was installed from the back to reduce heat losses. Through this door, the angle of the heat-absorbing surface was changed and the solar collector was cleaned of dust. The cover of each solar collector was manufactured using seven bars made of steel, the length of each of them is 220 cm, and it is inclined with a circular arc of 50 cm in radius, which was used as a structure for fixing the acrylic sheets on it.



1	Metal foam absorber plate	6	MDF wood panel
2	Collector roof	7	Tire
3	PVC tower	8	Steel cable
4	Separate wood panel	9	PVC ring
5	Flat plate absorber	10	Steel ring

(a) The SUTS Parts

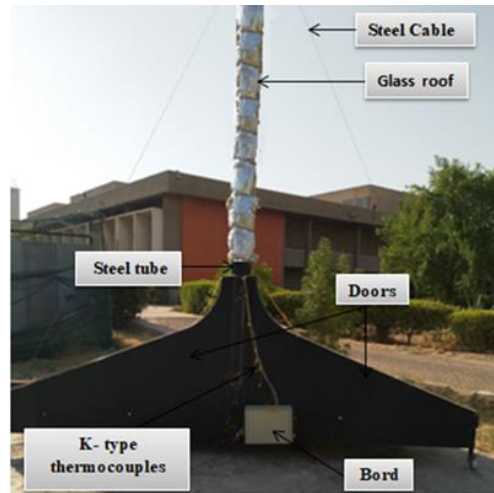


(b) The SUTS dimensions (All dimension in centimeter)

Figure 4. Schematic of the experimental device



(a) The SUTS Photograph (front view)



(b) The SUTS photograph (backside)

Figure 5. The experimental apparatus photograph

3.2. Construction, and Bonding of Copper Foam Panels

Fig. 6 and Fig.7 show the copper foam panels that have been installed and bonded to the quarter-circular solar collector structure. The volume of each porous panel is $(50 * 50 * 10)$ cubic centimeters. The panels were arranged regularly to cover the solar collector structure area of 24040.6 cm^2 . Copper foam panels were cut and installed around the perimeter of the structure using a steel saw to cover the arc of the solar collector structure. The panels are installed and joined together tightly and strongly at a distance of 1 cm to cover the total area of the base of the solar collector structure.

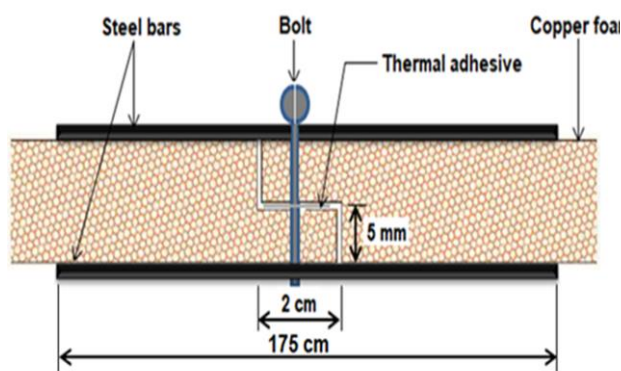


Figure 6. Schematic drawing metal foam absorption overlap

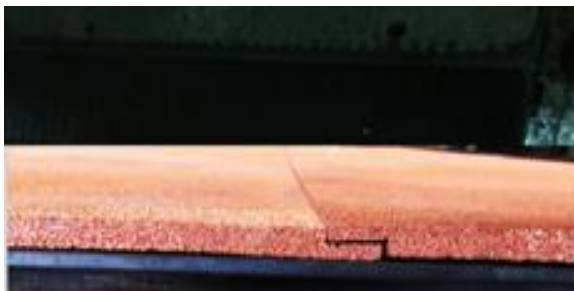


Figure 7. Method of overlapping between the copper foam Panels

An adhesive and thermally conductive material was used in the overlapping areas of the copper foam panels to increase the pressure strength of

the connection between the panels in the connection areas, as shown in Fig. 6. The final design of the porous copper absorbent foam surface is shown in Fig. 8.



Figure 8. Final design of copper foam absorption plate

3.3. Updraft Solar Tower Tube

A 5 mm thick PVC pipe was used to simulate the solar tower as shown in Fig. 1 and Fig. 2. Four steel cables with a thickness of 5 mm were used to hold and prevent the movement of the solar tower during the increase in wind speed. A wooden panel with a thickness of 2 cm was fixed along the middle of the solar tower to connect with the wood panel installed at the center of the semi-circular solar collector structure to form two fully separated SUTS as shown in Fig. 9. The solar tower was isolated from the outside using glass wool, which has a low thermal conductivity of 0.46 W / m. K , to prevent and reduce heat leakage to the outside.

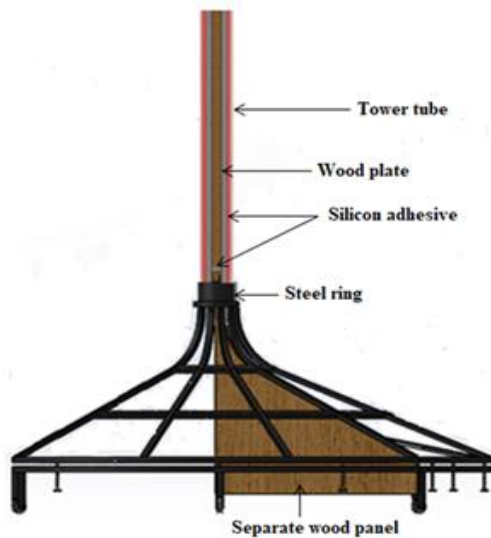


Figure 9. Schematic drawing of tower tube installing

3.4. Experimental Procedure

Experimental tests were conducted from 9:00 AM until 3:00 PM, where practical readings were taken every hour. Some important measures have been taken before taking the practical readings, the most important of which are:

1. Removing the dust from the metal foam and flat absorber plates by using the air blower.
2. Cleaning the transparent acrylic sheets (collector roof) by removing dust and dirt that accumulate on them.
3. Re-positioning the SUTS every hour to track the direction of the thermal solar radiation with the use of the steel strip installed above the collector roof along the separated section between the two-quarter circular collectors.
4. Finally, the readings of the thermocouples were taken using a data logger device.

3.5. Experimental Calculation

The objective of the experimental calculations is to analyze the performance of SUTS in the presence and absence of porous copper foam as an endothermic surface.

The output power of the solar updraft tower system can be calculated through the following equation [27];

$$P_{out} = \dot{Q}_{solar} * \eta_c * \eta_t * \eta_{turbine} \quad (14)$$

Due to the turbine was not used in the current work, so the equation 14 became as follows;

$$P_{out} = \dot{Q}_{solar} * \eta_c * \eta_t = \dot{Q}_{solar} * \eta_{plant} \quad (15)$$

The intensity of the solar radiation can be written as;

$$\dot{Q}_{solar} = IA_c \quad (16)$$

The below equation was used to determine the useful gain of energy as;

$$\dot{Q}_u = \dot{m}c_p(T_{c,o} - T_{amb.}) \quad (17)$$

\dot{m} is the rate of air mass flow and can be calculated as follows;

$$\dot{m} = \rho_t v_t A_c \quad (18)$$

The thermal efficiency η_c for each solar collector was calculated as;

$$\eta_c = \frac{\dot{Q}_u}{\dot{Q}_{solar}} \quad (19)$$

The efficiency of the solar tower was calculated from the following equation;

$$\eta_t = \frac{g.H_t}{c_p.T_{amb}} \quad (20)$$

The pressure resulting from the temperature difference between the air inlet of the solar tower and the air surrounding the tower can be calculated from the following equation:

$$\Delta p = g \int_0^{H_t} (\rho_{amb} - \rho_{c,o}) dy \quad (21)$$

As a result of isolating the solar tower from its surroundings, Equation 21 becomes as follows;

$$\Delta p = g(\rho_{amb} - \rho_{c,o})H_t \quad (22)$$

The overall output power can be calculated from the below equation;

$$P_{out} = \eta_t \times \dot{Q}_u = \frac{g.H_t}{C_p.T_{amb}} \times \dot{Q}_u \quad (23)$$

by substituting equations 17 and 18 into equation 23, the equation becomes as;

$$P_{out} = \frac{\rho_t v_t A_c g.H_t (T_{c,o} - T_{amb})}{T_{amb}} \quad (24)$$

The Boussinesq estimation gives the relation between the density and temperature as;

$$\frac{T_{c,o} - T_{amb}}{T_{amb}} \cong \frac{\rho_{amb} - \rho_{c,o}}{\rho_{c,o}} \quad (25)$$

Where, $(T_{c,o} - T_{amb})$ represents the difference in temperature between the exit of the collector (tower inlet) and ambient temperatures. So, equation 24 can be re-written to become as;

$$P_{out} = v_t A_c \Delta p \quad (26)$$

4. Results and Discussions

The experimental and numerical results were analyzed and discussed to evaluate the performance of the solar tower system using porous copper foam and conventional absorbent plate.

4.1. Numerical Results

The different cases in the numerical results depended on the investigated parameters, geometry, and weather data that were used in the experimental part. The numerical results are verified through the experimental tests carried out under the same conditions.

4.1.1. Temperature contours

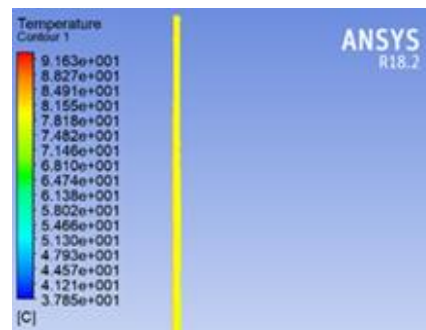
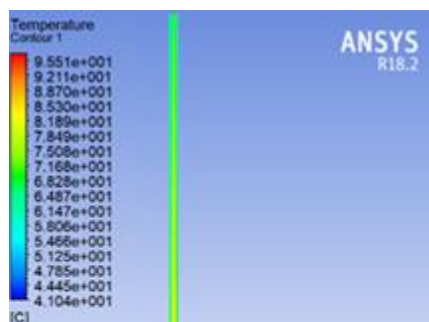
The comparison between the flat absorber plate and porous copper foam absorber surface is

shown in Fig. 10 for the inclination angle $\beta=0^\circ$ and heat flux of 915 W/m^2 . The figure shows that the magnitude of the temperature contours of the traditional absorbent plate is higher than that of the porous copper foam.

Fig. 11 shows a comparison between a flat absorber plate and a copper metal foam absorber plate for the inclination angle $\beta=18^\circ$ and heat flux of 935 W/m^2 . It is noted from the figure that the mechanism of heat transfer is more efficient with the metal foam absorber plate. Also, the thermal boundary layer with a metal foam absorber plate is developed along the upper and lower surfaces of the absorber plate. Whereas, with a flat absorber plate, the thermals boundary layer is mainly developed along the upper absorber surface. As a result, the presence of the copper metal foam as a heat absorbent plate caused to increase in the heat transfer significantly.

4.1.2. Air streamline

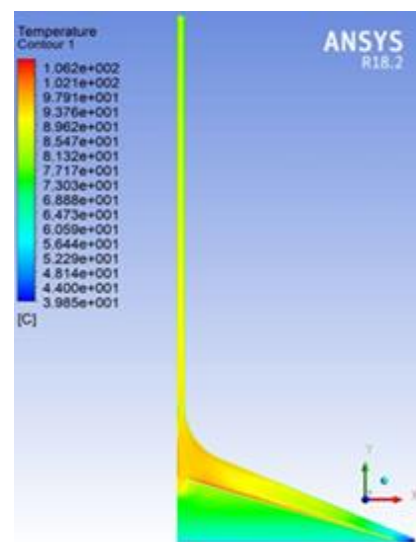
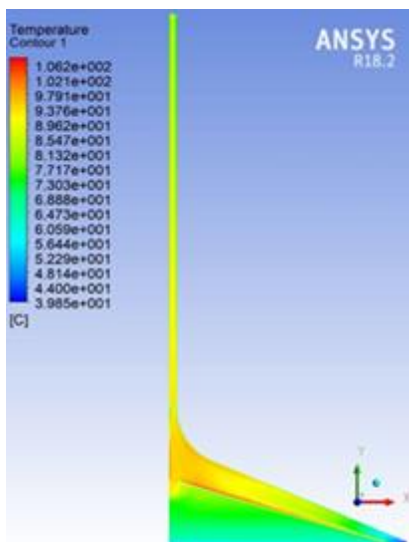
Fig.12 presents the air streamline with a flat and metal foam absorber plate at $(\beta=0^\circ, I=915 \text{ W/m}^2)$. A general behavior can be deduced from the figure that the buoyancy effect produced circulated streamlines with continuous returned air in the collector space using a flat absorbent plate. The behaviors represent the defect in the flat plate absorber collector setup which caused considerable losses in the total power production. In the case of the copper foam as an absorbent surface, the buoyancy force induced the streamlines to move towards the exit section which indicates an enhancement in the performance of the heat transfer compared with traditional absorbent plate.



(a) Temperature Contours for Flat Absorber

(b) Temperature Contours for MF Absorber Plate

Figure10. Temperature Contours of SUTS for flat plate and MF Absorber Plate at $\beta=0^\circ$, $I=915 \text{ W/m}^2$



(a) Temperature Contours for Flat Absorber Plate

(b) Temperature Contours for MF Absorber Plate

Figure11. Temperature Contours of SUTS for flat plate and MF Absorber Plate at $\beta=18^\circ$, $I=935 \text{ W/m}^2$

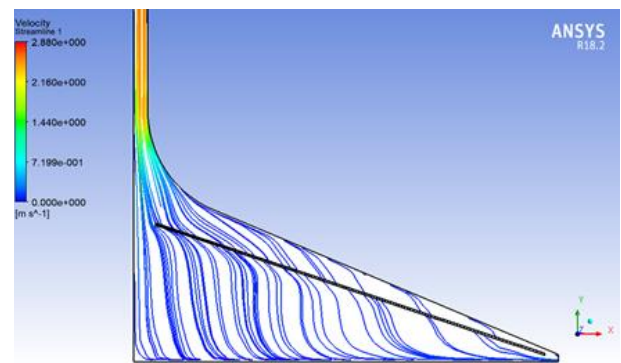
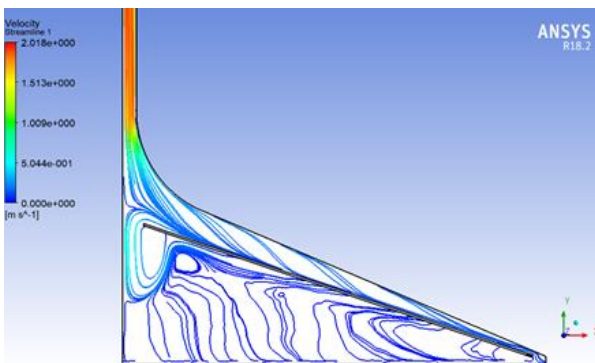
Fig. 13 shows the air streamline versus flat and metal foam absorber plates at ($\beta=18^\circ$ and $I=935 \text{ W/m}^2$). It is noted from the figure that in the case of a flat plate absorber plate is inclined at an angle, the circulations begin to decrease and become weaker, and it is noticed that the lower part of the flat absorber plate has large circulations compared to the top part of the plate, and this is because the flat plate is impermeable.

In the case of the copper foam absorber plate, there are no circulations and the streamlines are smooth towards the exit section through the collector absorber plate because the collector absorber plate is considered permeable. There is an enhancement in the airflow velocity for porous copper foam as an absorbent plate about 43.6% if compared with the case of a flat absorbent plate.



(a) Air streamline for flat absorber plate

(b) Air streamline for MF absorber plate

Figure 12. Air velocity streamline of SUTS for flat and MF absorber plate at $\beta=0^\circ$ 

(a) Air streamline for flat absorber plate

(b) Air streamline for MF absorber plate

Figure 13. Air velocity streamline of SUTS for flat and MF absorber plate at $\beta=18^\circ$

This indicates that with an increase in the inclination angle, the copper foam plate is better than the flat plate.

4.13. Average air velocity at the tower inlet

Fig. 14 shows the air velocity average at tower inlet for flat plate and copper foam at $\beta=0^\circ$ in Fig. 14a and $\beta=18^\circ$ in Fig. 14b. In general, the air velocity average at the tower inlet using a flat and copper foam plate inside the collector increases as a result of the increase in the solar radiation intensity, but after noon the radiation intensity is

decreased causing to reduce the air velocity gradually.

From the figure, it can be noticed that average of the air velocity using a copper foam plate is higher than that of a flat absorber due to the heat absorbent surface area of the collector causing to increase in the rate of heat transfer at fluid moving towards the tower which causes a higher the air velocity at the entrance of the solar tower. Thus, the enhancement of heat transfer can be conducted by using the porous metal foam as an absorbent plate.

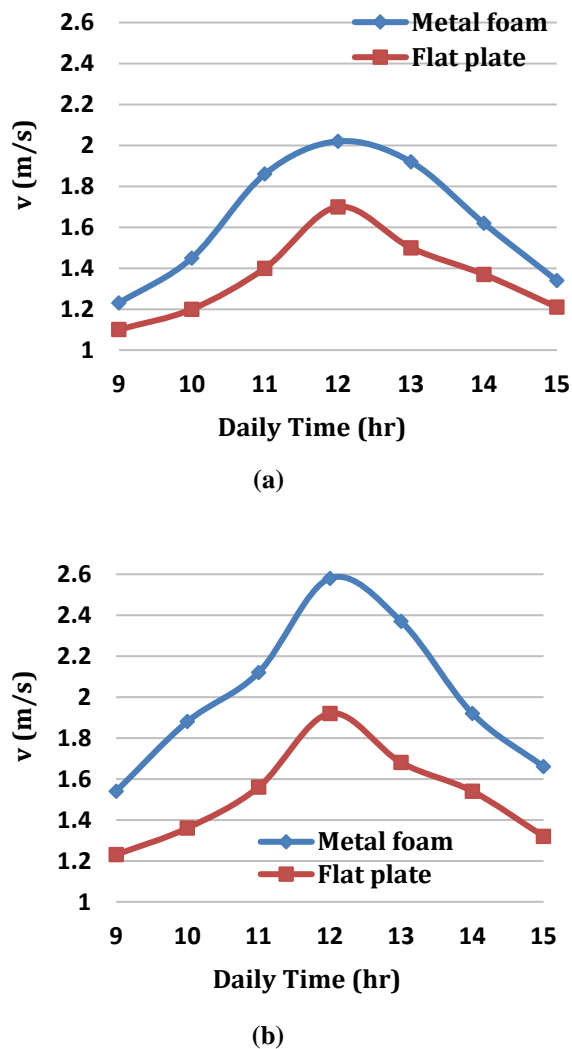


Figure 14. Tower inlet velocity for flat and MF absorber plate with the time at (a) $\beta = 0^\circ$ & (b) $\beta = 18^\circ$

4.2. Experimental Results

4.2.1. Surface absorber plate temperature

Fig. 15 shows the comparison of the hourly temperature distribution average for flat and copper foam plate at $\beta = 0^\circ$ in Fig. 15a and $\beta = 18^\circ$ in Fig. 15b. In general, the average absorber plate temperature increase with an increase in the solar intensity, but after noon the solar intensity is decreased causing to reduce the absorber plate temperature gradually. It is also noted that the average absorption temperature increases at the inclination angle of $\beta = 18^\circ$ compared with $\beta = 0^\circ$ due

to the increase in the thickness of the thermal boundary layers for a higher inclination angle. The maximum average plate temperature difference is recorded between the flat and copper foam absorbent plates reached 15.3 at $\beta = 0^\circ$, while 7.4 at $\beta = 18^\circ$.

4.2.2. Air flow temperature distribution

Fig. 16 shows an hourly variation of the average air temperature measured within the collector at the upper of the flat and copper foam plate at $\beta = 0^\circ$. It is noted that the variation of the average air temperature with a copper foam plate is higher than that of a flat absorber plate which indicates that the thermal boundary layers thickness is higher in the case of the copper foam plate as an increase of the induced airflow. The highest value of average air temperature is 72.2°C with a metal foam absorber plate and 63.8°C with a flat absorber plate.

Fig. 17 presents the comparison between an hourly variation of the average of the air temperature measured within the collector above and below the flat plate and copper foam at $\beta = 18^\circ$. It can be noted that the average air temperature is above and below the copper foam surface is higher than that of the flat absorber plate which gives evidence that the heat transfer process in the presence of the metal foam absorber plate is better than of the flat plate. It can also be seen that the average air temperature above the absorbent plate is higher than below the absorbent plate due to the development and the thickness of the boundary layer on the upper surface is greater than that of the lower surface as a result of the buoyancy effect.

4.2.3. Air velocity at tower inlet

The variation in air velocity at the entrance to the tower every hour with flat and copper foam plates is shown in Fig. 18 (a&b) at ($\beta = 0^\circ$ and $\beta = 18^\circ$) respectively. It is seen from the figure that the

copper foam as an absorbent plate caused an increase in air velocity significantly compared to the flat plate. The reason for this is due to the pores increase the surface area of heat transfer causing to enhance the fluid's velocity toward the entrance of the solar tower. Also, it was noted that the changing of the inclination angle from ($\beta=0^\circ$ to $\beta=18^\circ$) caused a clear increase in the airflow velocity, especially with the presence of the copper foam plate due to the increased influence of the buoyancy force for higher inclination angles. The maximum enhancement of the air velocity with and copper foam plate to about 25% compared with a flat plate at $\beta=0^\circ$, while to about 57.6% at $\beta=18^\circ$.

.42.4. Solar collector thermal efficiency

The thermal efficiency of the collector with flat and copper foam absorption plates can be illustrated in Fig. 19 (a & b) for ($\beta=0^\circ$) and ($\beta=18^\circ$) respectively. It is noted from the figures that the presence of the copper foam plate increases the collector thermal efficiency significantly, especially with the inclination angle from ($\beta=0^\circ$ to $\beta=18^\circ$) compared with the conventional flat plate. The maximum thermal efficiency performance of the collector is recorded using the flat and metal foam absorbent plates at $\beta=0^\circ$ (17.6% and 21.9 %) respectively, while at $\beta=18^\circ$ is recorded (22.4% and 46.6%) respectively.

.42.5. Airflow power (Power output)

Fig. 20 presents the variation of the power output versus time with flat and metal foam absorber plates at $\beta=0^\circ$ and $\beta=18^\circ$ respectively. It is noted that the power output increases with an increase in the inclination angle ($\beta=18^\circ$) due to an increase in the air velocity flow as an increase in

the buoyancy effect. The power output has larger values with the copper foam absorbent than with the flat absorbent plate. The maximum power output was recorded with a metal foam absorber plate to rise about 47.3% at $\beta=18^\circ$. This is evidence that the use of metal foam absorption gives good results in the improvement of the SUTS performance.

4.3. Comparison with Previous Experimental Works

Comparison of current empirical data with other research is based on the concept of the general disposition of some of the parameters studied of the performance of SUTS. Fig. 21 shows a comparison of air velocity at the entrance of the tower against time between the present study and the previous experimental result [28]. The comparison gave an acceptable result in the trend behavior, and this is evidence of the correctness of the results obtained.

4.4. Comparison between the Experimental and Numerical Results

In this section, the comparison between experimental and numerical work using flat and copper foam absorbent plates of airflow velocity at the tower inlet with ($\beta=18^\circ$). Fig. 22 shows the values that obtained experimentally are compared with those obtained numerically. It can be noticed that the results have the same trends but there is some difference between them. The maximum error of airflow velocity at the tower inlet is about 27.1% in the case of a flat plate absorber plate, and about 18.5% if using a metal foam absorbent plate during the measurements and theoretical assumptions that are used in the numerical simulations. The reason for this difference is due to the possibility of heat loss, and errors that may occur.

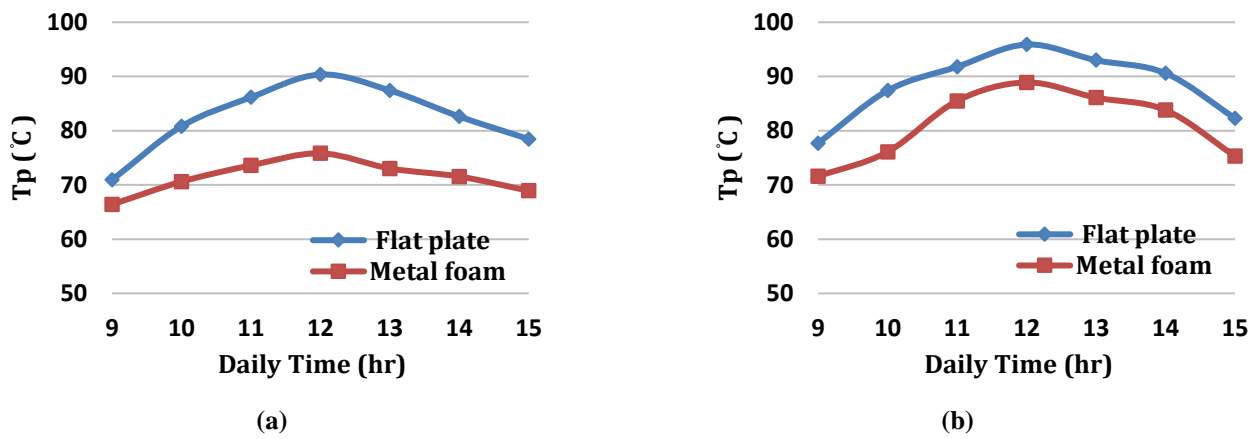


Figure 15. Average wall temperature for flat and MF absorber plate with the time at (a) $\beta = 0^\circ$ & (b) $\beta = 18^\circ$

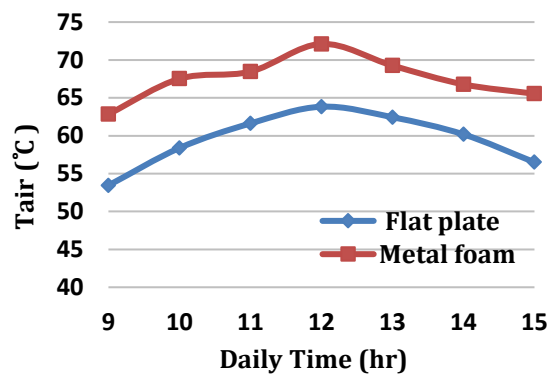


Figure 16. Change of mean air temperature from the above flat and absorption plate with time at $\beta = 0^\circ$

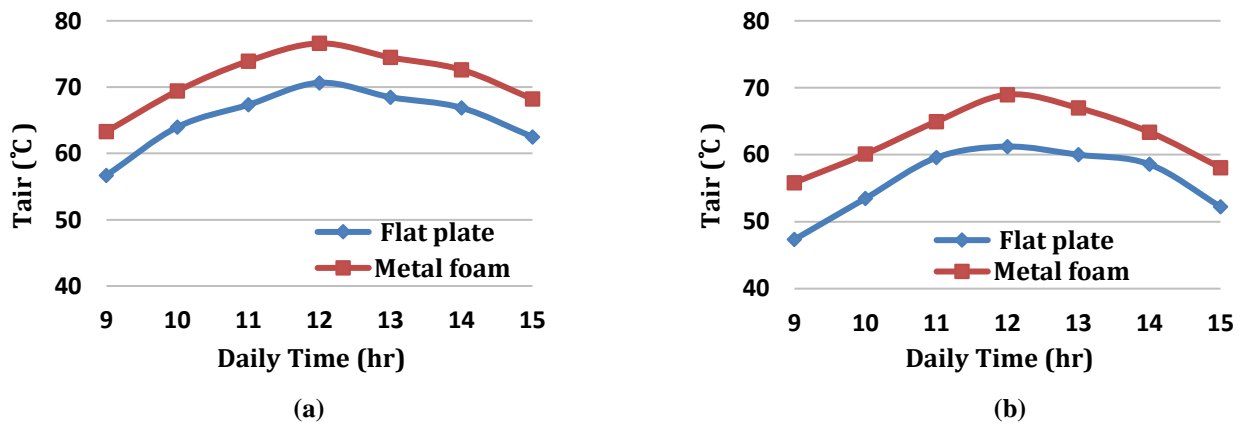


Figure 17. Change of mean air temperature from (a) above & (b) below the flat and MF absorber plate with time at $\beta = 18^\circ$

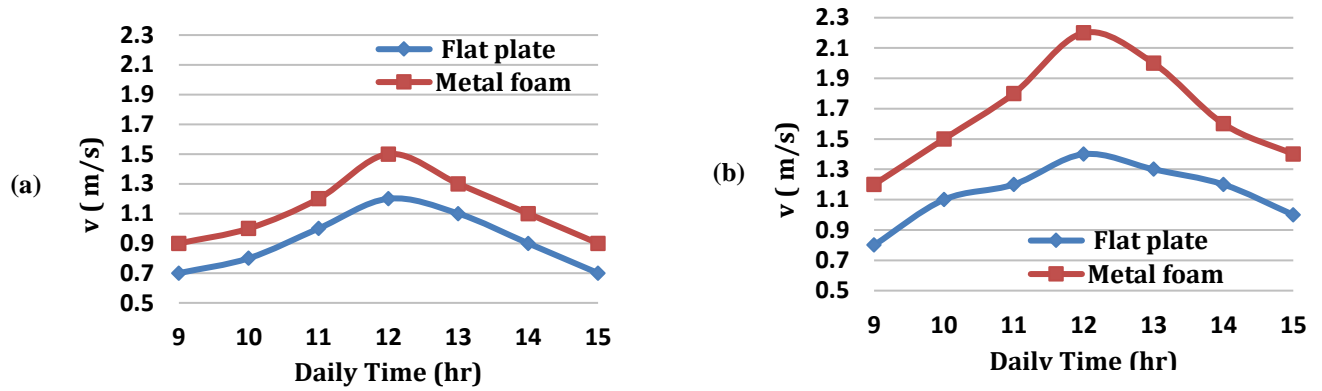


Figure 18. Change of air velocity at the tower entrance with time for flat and MF absorption at (a): $\beta=0^\circ$ & (b): $\beta=18^\circ$

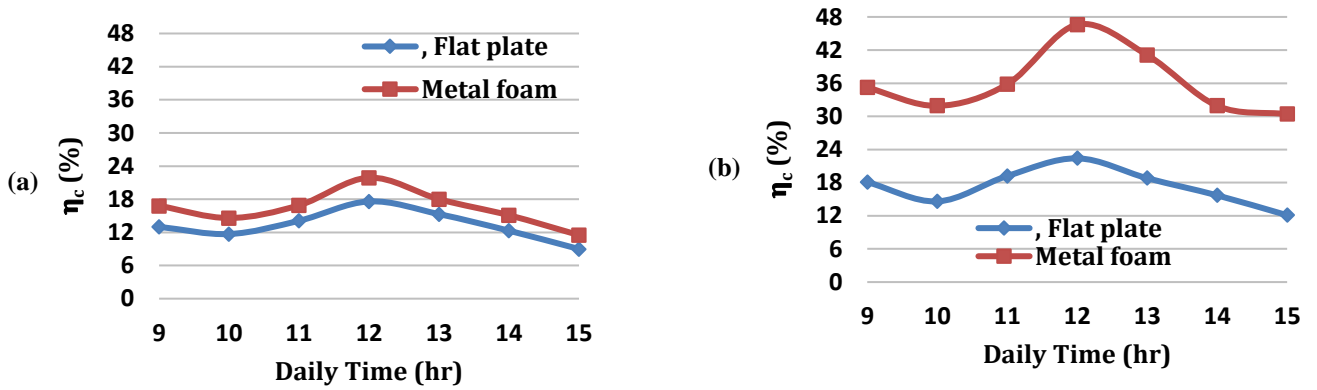


Figure 19. Variation of collector thermal efficiency for flat plate and MF absorber plate with the time at (a) $\beta=0^\circ$ & (b) $\beta=18^\circ$

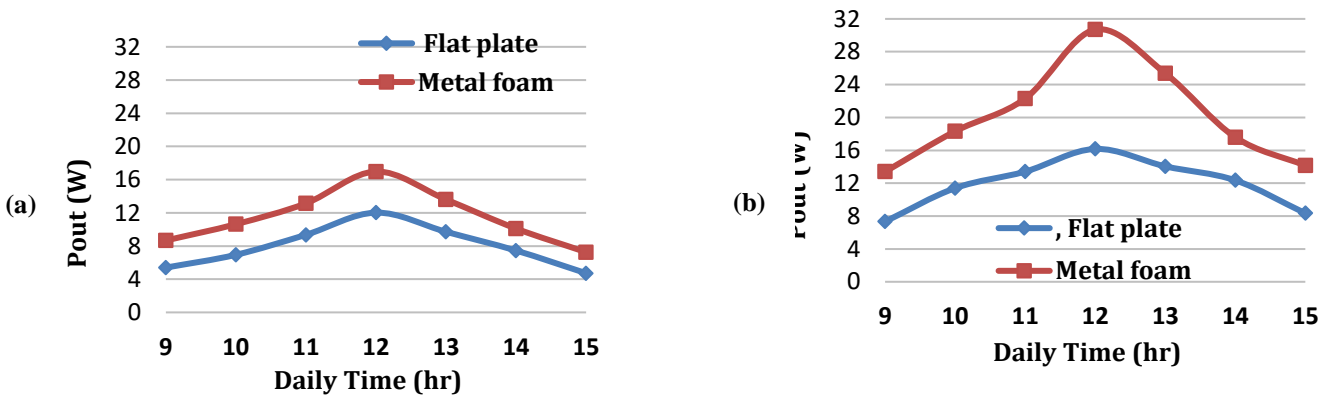


Figure 20. Change of the power output for traditional plate and MF absorber plate with the time at (a) $\beta=0^\circ$ & (b) $\beta=18^\circ$

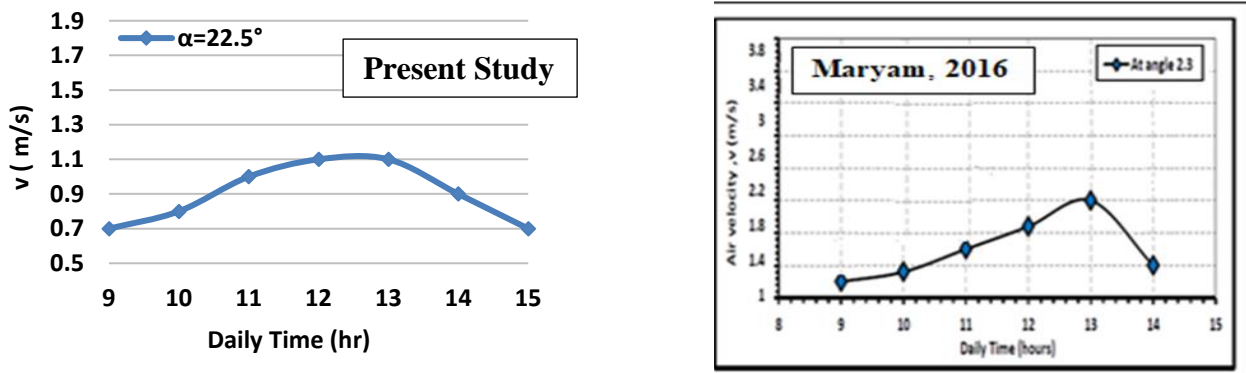


Figure 21. Comparison of air velocity at the tower inlet with time between the present study and previous experimental result, Maryam [20]

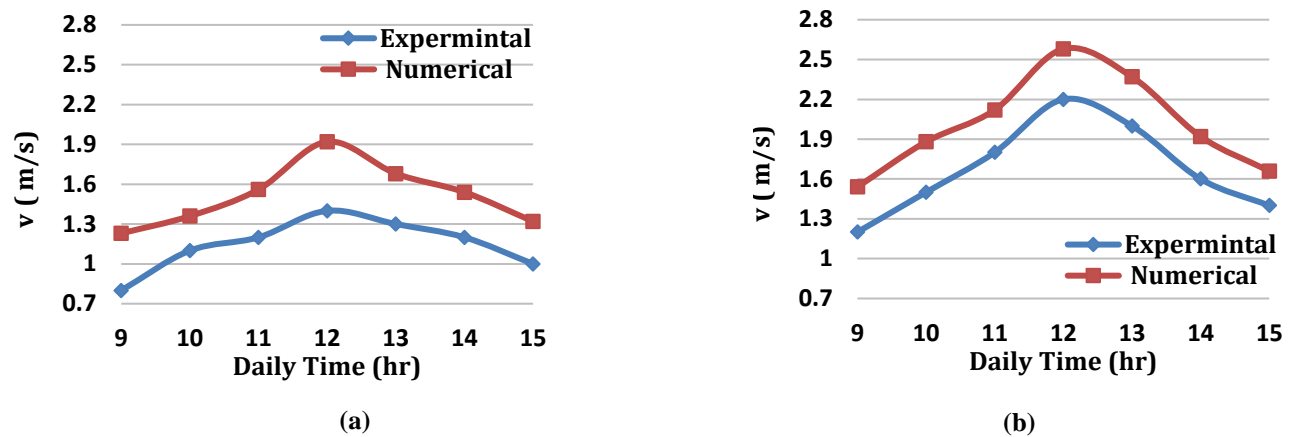


Figure 22. Change of air velocity at the entrance of the tower with time at ($\beta=18^\circ$) for (a) flat absorber plate and (b) MF absorber plate

5. Conclusions

The tests of numerical and experimental were carried out to validate an enhancement of the characteristics of heat transfer and SUTS performance using a flat plate and copper foam as a collector absorbent plate. The numerical and experimental tests are carried out on the free convective heat transfer with two inclination angles of 0° and 18° for the copper absorber plate and conventional flat plate. The conclusions can be summarized as follows:

1. The surface temperatures of the copper foam absorption plate are less than those of the flat absorption plate.
2. The airflow temperature of the copper foam absorption is higher than that of a conventional flat plate.
3. The enhancement in air flow velocity at tower exit for metal foam absorber plate to about 40.2% and 43.3% if compared to flat plate absorber with same angles inclining of 0° and 18° respectively.
4. The values of the air temperature difference (ΔT) for copper foam plate are higher than that of a flat plate at each inclination angle.

5. The thermal efficiency with the copper foam plate is enhanced to about 21.9% at $\beta=0^\circ$ and to about 46.6% at $\beta=18^\circ$ compared with a flat absorption plate.
6. The power output with the copper foam plate is enhanced to about 29.2% at $\beta=0^\circ$ and to about 18.3% at $\beta=18^\circ$ compared with a flat absorption plate.

Numerical simulation results and experimental data show that using a copper foam absorption surface inside the SUTS is an effective way to enhance the heat transfer properties and collector thermal performance under Iraqi climate conditions, especially with higher solar irradiance intensity and with angle inclining of the collector absorber plate.

Acknowledgments

This scientific paper is part of a Ph.D. dissertation at the Mechanical Engineering Department, College of Engineering, Baghdad University, and the authors express their deep gratitude to each person who contributed to the completion of this research.

Conflict of interest

The authors of this manuscript declare that there are no conflicts regarding the manuscript publication.

Author Contribution Statement

The author Sarmad A. Abdul Hussein worked on developing the research methodology by reviewing and evaluating the proposed indicators. The author Mohammed A. Nima proposed the idea of research and supervised it. All indications have been discussed by the two authors to contribute to the final form of the manuscript

List of Symbols

a	Permeability of the metal foam (m^2)
A	Cross section area (m^2)
C	Inertial coefficient
C_F	Inertial drag factor
C_P	Specific heat at constant pressure ($J/kg.K$)
d_f	Ligament diameter of the metal foam (m)
d_p	Pore diameter of the metal foam (m)
D	Diameter (m)
E	Total energy (kJ)
G	Production of turbulent kinetic energy
H	Height (m)
I	Solar radiation intensity (W/m^2)
$I(r, s)$	Radiation intensity (W/m^2)
\vec{j}	Unit vector in the y-direction
k	Thermal conductivity ($W/m.K$)
\dot{m}	Air mass flow rate (kg/s)
p	Pressure (Pa.)
P_{out}	Power output (W)
r	Radius (m)
t	Time (s)
T	Temperature ($^{\circ}C$)
v	Air velocity (m/s)
\dot{Q}	Heat flux (W)
S	Modulus of mean strain rate tensor
w	Width (m)

Greek Letters

α_f	Thermal diffusivity of the working fluid
β	Absorber plate inclination angle (Degree)
ε	Porosity, Emissivity
η	Thermal efficiency (%)
μ	Dynamic Viscosity
ρ	Density (kg/m^3)
σ	Stefan – Boltzmann Constant ($W/m^2.K^4$)

Subscript

amb	Ambient
c	Collector
eff	Effective
atm	Atmosphere
i	Inlet
ave.	Average
o	Outlet
p	Plate
t	Tower

Abbreviation

Do	Radiation desecrate ordinate
Conv.	Convection
MF	Metal foam
Rad.	Radiation
SUTS	Solar updraft tower system

References

1. Kasaeian A., Ghalamchi M. (2014). "Simulation and optimization of geometric parameters of a solar chimney in Tehran". Energy Convers Manage, 83, pp. 28–34. <https://doi.org/10.1016/j.enconman.2014.03.042>
2. Kalasha S., Naimeh W. (2014). "Experimental investigation of a pilot sloped solar updraft power plant prototype performance throughout a Year". Energy Procedia, 50, pp. 624-633. <https://doi.org/10.1016/j.egypro.2014.06.077>

3. Hamdan M.O. (2011). "Analysis of a solar chimney power plant in the Arabian Gulf region". *Renewable Energy*, 36, 2593–2598. <https://doi.org/10.1016/j.renene.2010.05.002>
4. Zhou X.P., Yang J.K., Xiao B., Hou G.X. (2007). "Experimental study of temperature field in a solar chimney power setup". *Appl. Therm. Eng.*, 27, pp. 2044–2050. <https://doi.org/10.1016/j.applthermaleng.2006.12.007>
5. Mohammed A. Nima, Ali M. Ali. (2017). "Effect of Metal Foam Insertion on Thermal Performance of Flat-Plate Water Solar Collector Under Iraqi Climate Conditions" *Arab J Sci Eng*, 42, pp. 4863–4884. <https://doi.org/10.1007/s13369-017-2683-z>
6. Abbas Husain Hajeej. (2016). "Mixed Convection Heat Transfer Enhancement in a Channel by Using Metal Foam Blokes". M.Sc. Thesis, University of Baghdad, Iraq. <https://doi.org/10.31026/j.eng.2016.05.10>
7. Zhou X.P., Wang F., Fan J.A. (2010). "Performance of solar chimney power plant in Qinghai- Tibet Plateau". *Renew Sustain Energy*, Rev 1: pp. 2249–55. <https://doi.org/10.1016/j.rser.2010.04.017>
8. Zhou X.P., Wang F., Ochieng R.M. (2010). "A review of solar chimney power technology". *Renew Sustain Energy*, Rev 14: pp. 2315–38. <https://doi.org/10.1016/j.rser.2010.04.018>
9. Manal H. Jassim, Ali Reyadh Waheed. (2014). "Implementation of Solar Energy Tracking System". *Journal of Engineering and Sustainable Development (JEASD)*, Vol. 18, No.4, pp. 124-140.
10. Johannes Petrus Pretorius. (2004). "Solar Tower Power Plant Performance Characteristics". M.Sc. Thesis, University of Stellenbosch, Private Bag X1, 7602 Matieland, South Africa.
11. Abdel Hamid Boualit, Saleh Larbi, Amor Bouhdjar. (2010). "Finite Element Analysis of Laminar Flow in Solar Chimney". Séminaire International sur le Génie Climatique et l'Energétique, SIGCLE.
12. Chang Xu, Zhe Song, Leader Chen, Yuan Zhen. (2011). "Numerical investigation on porous media heat transfer in a solar tower receiver". *Renewable Energy*, Vol. 36, pp. 1138-1144. <https://doi.org/10.1016/j.renene.2010.09.017>
13. Elizabeth Marie Heisler. (2014). "Exploring Alternative Designs for Solar Chimneys Using Computational Fluid Dynamics". M.Sc. Thesis, Virginia Polytechnic Institute and State University.
14. Ehsan Gholamalizadeh, Man-Hoe Kim. (2016). "CFD computational fluid dynamics analysis of a solar-chimney power plant with inclined collector roof". *Energy*, Vol.107, pp. 661-667. <https://doi.org/10.1016/j.energy.2016.04.077>
15. Ayoob K. Jasim, Basim H. Abood, Mohammed H.Alhamdo. (2021). "Investigative Study of Thermal Performance of Thermosyphon Solar Collecto". *Journal of Engineering and Sustainable Development*, Vol. 25, No. 02, pp. 46-57. <https://doi.org/10.31272/jeasd.25.2.6>
16. Miqdam Tariq Chaichan. (2011). "Basement Kind Effects on Air Temperature of a Solar Chimney in Baghdad - Iraq Weather". *Al-Khwarizmi Engineering Journal*, Vol. 7, No. 1, pp. 30 – 38. <http://www.nitropdf.com/>
17. Mohammed H. Alkhafaji, Basim H. Abood, Mohammed H. Alhamdo. (2021). "Temperature Distribution within the Rising

- Pipe in Flat Plate Solar Collector*". Journal of Engineering and Sustainable Development, Vol. 25, No. 05, pp. 56-66. <https://doi.org/10.31272/jeasd.25.5.6>
18. Mehrdad Ghalamchi, Alibakhsh Kasaeian, Mehran Ghalamchi, Alireza Hajiseyed Mirzahosseini. (2016). "An experimental study on the thermal performance of a solar chimney". Renewable Energy, Vol. 91, pp. 477-483. <https://doi.org/10.1016/j.apenergy.2013.09.022>
 19. Carl F. Kirstein (2006). "Flow through a Solar Chimney Power Plant Collector-to-Chimney Transition Section". Journal of Solar Energy Engineering (ASME), Vol. 128, pp. 312-317. <https://doi.org/10.1115/1.2210502>
 20. Aseel K. Shyaa, Rafea A. H. Albaldawi, Maryam Muayad Abbood. (2016). "Experimental and Numerical Study of Collector Geometry Effect on Solar Chimney Performance". Al-Khwarizmi Engineering Journal, Vol. 12, No. 4, pp. 59-71. <https://doi.org/10.22153/kej.2016.05.002>
 21. Mohammed A. Aurybi, Hussain H. Al-Kayeim, Syed I. U. Gilani, and Ali A. Ismaeel. (2016). "Mathematical Modeling to Evaluate the Performance Enhancement of Solar Updraft Power Plant by External Heat Source". ARPN Journal of Engineering and Applied Sciences, Vol. 11, NO. 20, pp. 12128-12133.
 22. Buonomo B., di Pasqua A., Ercole D., Manca O. (2019). "The effect of PPI on thermal parameters in compact heat exchangers with aluminum foam". IOP Conf. Series: Journal of Physics: Conf. Series 1224, 012045. <https://doi.org/10.1088/1742-6596/1224/1/012045>
 23. Gue C.X., Zhang W.J., and Wang D.B. (2014). "Numerical investigation of heat transfer enhancement in latent heat storage exchanger with paraffin/graphite foam". 10th Int. Conf. on Heat Transfer, Fluid Mechanics and Thermodynamics, 14 – 26. <http://hdl.handle.net/2263/44539>
 24. Bergman T., Lavine A., Incropera F., and Dewitt D. (2011). "Fundamentals of Heat and Mass Transfer". 7th ed. John Wiley & Sons.
 25. Sinan Abdul Ghafar Ali. (2011). "Study the Effect of Upstream Riblet on Wing-Wall junction". M.Sc. Thesis, University of Technology, Iraq.
 26. Ghaffari, A., Mehdipour, R. (2015). "Modeling and Improving the Performance of Cabinet Solar Dryer Using Computational Fluid Dynamics". International Journal Food Engineering, Vol. 11, No. 2, PP. 157–172. <https://doi.org/10.1515/ijfe-2014-0266>
 27. Jörg Schlaich, Rudolf Bergermann, Wolfgang Schiel, Gerhard Weinrebe (2005). "Design of Commercial Solar Updraft Tower Systems – Utilization of Solar Induced Convective Flows for Power Generation". Journal of Solar Energy Engineering (ASME), Vol. 127, No. 117. <https://doi.org/10.1115/1.1823493>
 28. Maryam Muayad Abbood (2016). "Guide Vanes and Collector Geometry Effects on the Performance of Solar Chimney". M.Sc. Thesis, Al-Mustansiriyah University, Iraq.